European Association for the Development of Renewable Energies, Environment and Power Quality (EA4EPQ)

International Conference on Renewable Energies and Power Quality (ICREPQ'10)
Granada (Spain), 23th to 25th March, 2010

An innovative transmission mechanism applicable to variable speed wind turbines

G. S. Hwang[1], J. C. Lin[2], D. M. Tsay[2], J. H. Kuang[2] and T. L. Chern[3]

[1] Department of Computer Science and Information Engineering
Nanhua University
Chiayi 62248, (Taiwan)
Phone/Fax number: +886 5 2721001 ext. 50308, e-mail: gshwang@mail.nhu.edu.tw

[2] Department of Mechanical & Electro-Mechanical Engineering
[3] Department of Electrical Engineering
National Sun Yat-Sen University
Kaohsiung 80424, (Taiwan)

Abstract.

An innovative transmission mechanism, named as independently controllable transmission (ICT), is proposed in this study. While being applied to the variable speed wind turbines, the proposed ICT mechanism can transmit a steady-speed output, which is independently manipulated by a controller and completely not affected by the fluctuant speed of the rotor, to the generator to generate the electric power with constant frequency. The ICT mechanism is fundamentally composed of two sets of planetary gear trains and two sets of transmission-connecting members. Two prototypes of the ICT mechanisms are assembled to examine their kinematical characteristics and to demonstrate their feasibility in engineering applications.

Key words

independently controllable transmission (ICT), variable speed wind turbine, steady-speed, planetary gear train, transmission-connecting member.

1. Introduction

In comparison to a constant-speed wind turbine, a variable speed wind turbine has the advantages of increasing the amount of electricity generated by operating at higher aerodynamic efficiency and of mitigating fatigue loads caused by gusts. Consequently, the variable speed wind turbine system must become a key component of the wind energy system of the future given the prospects of improved performance and decreased costs [1-2].

In order to operate in wind speed variations, various electrical-mechanical designs have been proposed for the variable speed wind turbines. For examples, power electronic components are incorporated to change variable AC power to constant voltage and frequency. Adopting a back-to-back configuration with two voltage source converters, Pucci and Vitale present a high performance wind generator with induction machine [3]. In a variable speed wind turbine with a pitch control system, which regulates the effective rotor blade angle, optimum power can be obtained by using appropriate control methods [4-6]. Mangialardi and Mantriota propose a wind power system equipped with a continuously variable transmission to achieve high efficiency levels [7]. Idan and Lior present the theory and design of a hybrid mechanical-electrical variable speed wind turbine transmission, and discuss a robust control solution for optimal power output [8]. Zhao and Maiβer propose an electrically controlled power splitting drive train for variable speed wind turbines [9]. Lahr and Hong present the usage of the cam-based infinitely variable transmission of ratcheting drive type in variable speed wind turbines [10]. Müller et al., analyze grid integration aspects of a new type of variable speed wind turbine, the directly coupled synchronous generator with hydro-dynamically controlled gearbox, and without the application of any power electronics converter [11].

In this study, an innovative mechanism with independently controllable power transmission and named as independently controllable transmission (ICT) is proposed. The ICT mechanism, which is independently controlled by a controller without any relevance to the angular velocity of the input power shaft, can produce a steady-speed at the output power shaft. Such an ICT mechanism can be applied to the variable speed wind turbines, which allow the turbine rotors to operate at maximum aerodynamic efficiency in accordance with the wind speed variations. The proposed ICT mechanism is fundamentally composed of two sets of planetary gear trains and two sets of transmission-connecting members, and without using any other additional sliding friction element. Finally, two prototypes of the proposed ICT mechanism are assembled to examine their kinematical characteristics and to demonstrate their feasibility in engineering applications.

2. Conception and Conformation of ICT Mechanism

The conceptual scheme of the ICT mechanism, as depicted in Fig. 1, is a mechanism possessing four rotational shafts with specific capabilities, i.e., to connect to the input power end, the output power end, the controller, and the free end, respectively. In a practical application, the input power can be obtained from a wind turbine, and the output end can transmit the power to a generator. A servomotor whose angular velocity is controllable can be served as the controller. The free end can be a secondary input or output end freely, depending on the configuration of the mechanism and the speed ratio between the input and output ends. The speed ratio between the output end and the controller is fixed at a constant ratio without any relevance to the speed of the input end. Therefore, the desired angular velocity of the output power shaft, no matter what the angular velocity of the input end is, can be obtained by the independent manipulation of the controller.

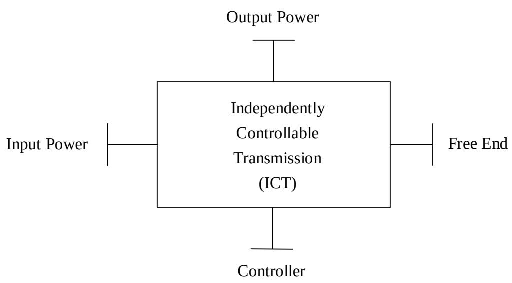

Fig. 1. Conceptual scheme of the ICT mechanism

The basic conformation of the ICT mechanism, as shown in Fig. 2, is primarily composed of two sets of planetary gear trains, denoted by *A* and *B* respectively, and two sets of transmission-connecting members, indicated by *D* and *E* respectively. As depicted by *AD*, *OP*, *AE* and *BD*, *CR*, *BE*, respectively, each planetary gear train has three rotational shafts, i.e., the shafts of the sun gear, the carrier and the central gear meshed with the planet gears. In each planetary gear train, two of the three shafts are connected to the transmission-connecting members *D* and *E*, respectively. For examples, the shafts *AD*, *BD* are connected to the transmission-connecting member *D*, and *AE*, *BE* to *E*, as shown in Fig. 2. The third shaft of the planetary gear train *A*, i.e., *OP*, can be connected to the output power end, and the third shaft of *B*, i.e., *CR*, can be connected to the controller. Finally, by means of the shaft *SD*, the transmission-connecting member *D* can be connected to the source of input power, on the other hand, the transmission-connecting member *E* is connected to the free end by shaft *SE*.

A. Establishment of Basically Kinematic Requirements

To achieve the capabilities of the proposed ICT mechanism, some basically kinematic requirements must be established. First, from the conception described previously, the relationship of the angular velocities between the two shafts *AD* and *BD* shown in Fig. 2, which are used to transmit the input power to the two sets of planet gear trains *A* and *B*, respectively, can be established as the following equation

$$n_{BD} = \alpha \, n_{AD} \tag{1}$$

where n denotes the angular velocity and its subscript indicates the rotational shaft, α is a constant multiple.

Second, since the angular velocity of the output end is independently manipulated by the controller without any relevance to the angular velocity of the input power end, the relationship of the angular velocities between the shafts connected to the output end and the controller, i.e., *OP* and *CR*, can be established as the following equation

$$n_{CR} = \beta \, n_{OP} \tag{2}$$

where β is a constant multiple.

Finally, the relationship of the angular velocities between the shafts *AE* and *BE* are established to be equal

$$n_{AE} = n_{BE} \tag{3}$$

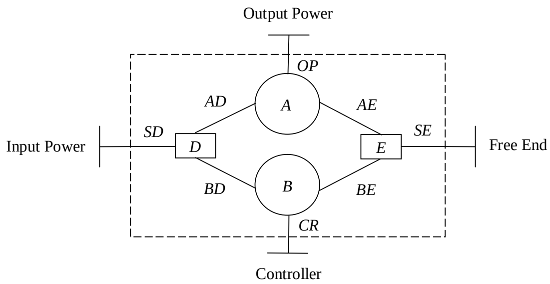

Fig. 2. Conformation of the ICT mechanism

B. Positive-Ratio Planetary Gear Train

The planetary gear train with positive-ratio drive train type, which will be used in the ICT mechanism, is shown in Fig. 3. The positive-ratio planetary gear train includes a sun gear member *ps*1 mounted on the rotational shaft *pss*1, a central gear member *ps*2 mounted on the rotational shaft *pss*2, at least one compound planet gear set with gears *pp*1 and *pp*2**,** which meshes with the sun gear *ps*1 and the central gear *ps*2, and a planet gear carrier member *pa*.

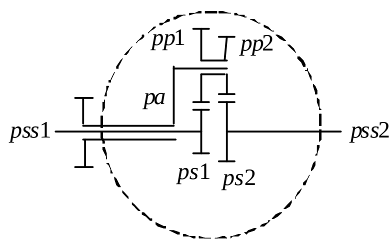

Fig. 3. Positive-ratio planetary gear train

A positive-ratio planetary gear train means that the shafts of the sun gear and the central gear, when the carrier is fixed, have the same direction of rotation. Therefore, its basic speed-ratio, which is defined as the ratio of the relative velocities between the shafts of the sun gear and the central gear, is consequently positive, moreover, the value of the basic speed-ratio cannot be equal to 1 [12]. In this positive-ratio planetary gear train, the rotational shafts *pss*1 and *pa* are a set of coaxial shafts, and *pss2* is a monoshaft. These three rotational shafts are the rotational shafts of each planetary gear train in the ICT mechanism, namely *AD*, *OP*, *AE*, or *BD*, *CR* and *BE*, as shown in Fig. 2, respectively.

From the above descriptions, the basic speed-ratio of the positive-ratio planetary gear train, denoted by i_0, can be expressed as the following equation

$$i_0 = \frac{n_{pss1} - n_{pa}}{n_{pss2} - n_{pa}} = \frac{N_{pp1} \times N_{ps2}}{N_{ps1} \times N_{pp2}} \tag{4}$$

where *N* is the teeth number of a gear and its subscript indicates the gear. By rearranging Eq. (4), the following velocity expressions of the rotational shafts *pps*2 and *pa* can be also respectively obtained

$$n_{pss2} = \frac{n_{pss1} - (1 - i_0) n_{pa}}{i_0} \tag{5}$$

$$n_{pa} = \frac{n_{pss1} - i_0 n_{pss2}}{1 - i_0} \tag{6}$$

C. Transmission-Connecting Member

The transmission-connecting member that can be provided to the usage in this study is shown in Fig. 4. This transmission-connecting member basically comprises the gear *cmg*1 mounted on the rotational shaft *cms*, which can be used to connect to the source of input power or the free end, and the gears *cmg*2 and *cmg*3 mounted on the shafts coming from the two planet gear trains *A* and *B*, respectively. The capability of shaft *cms* is similar to that of the shaft *SD* or *SE* shown in Fig. 2, and the shafts coming from the two planet gear trains *A* and *B* are just the shafts *AD*, *BD* or *AE*, *BE* shown in Fig. 2, respectively. One of the shafts respectively coming from the two planet gear trains is the outer shaft of a set of coaxial shafts, and the other is a monoshaft.

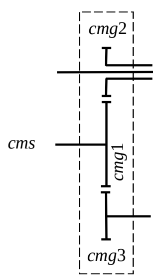

Fig. 4. Transmission-connecting member

D. Practical Arrangement of ICT Mechanism

According to the kinematic requirements and the conformation of the ICT mechanism, which are described in the previous section, a practical arrangement of the ICT mechanism is proposed and schematically shown in Fig. 5.

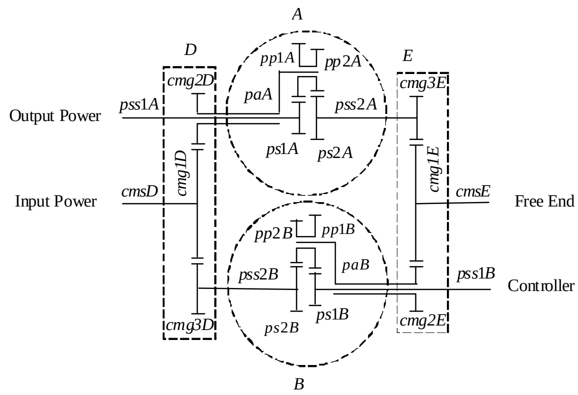

Fig. 5. A practical arrangement of the ICT mechanism

3. Kinematical Analyses of ICT Mechanisms

As schematically shown in Fig. 5, both the planetary gear trains *A* and *B* of the ICT mechanism are the positive-ratio types as shown in Fig. 3, and both the transmission-connecting members *D* and *E* are as shown in Fig. 4, respectively. The rotational shafts *cmsD* and *cmsE*, similar to the shafts *SD* and *SE* shown in Fig. 2, are connected to the input power end and the free end, respectively. The rotational shafts *pss*1*A* and *pss*1*B*, similar to the shafts *OP* and *CR* shown in Fig. 2, are connected to the output power end and the controller, respectively. Moreover, the functions and performances of the rotational shafts *paA*, *pss*2*A*, *pss*2*B* and *paB* will be also similar to those of the shafts *AD*, *AE*, *BD* and *BE* shown in Fig. 2, respectively. From the analyses described previously, Eqs. (1)-(6) can be rewritten as the following equations

$$\frac{n_{pss2B}}{n_{paA}} = \frac{N_{cmg2D}}{N_{cmg3D}} = \alpha \tag{7}$$

$$n_{pss1B} = \beta \, n_{pss1A} \tag{8}$$

$$n_{pss2A} = n_{paB} \tag{9}$$

$$i_{0A} = \frac{n_{pss1A} - n_{paA}}{n_{pss2A} - n_{paA}} = \frac{N_{pp1A} \times N_{ps2A}}{N_{ps1A} \times N_{pp2A}} \tag{10}$$

$$i_{0B} = \frac{n_{pss1B} - n_{paB}}{n_{pss2B} - n_{paB}} = \frac{N_{pp1B} \times N_{ps2B}}{N_{ps1B} \times N_{pp2B}} \tag{11}$$

$$n_{pss2A} = \frac{n_{pss1A} - (1 - i_{0A}) n_{paA}}{i_{0A}} \tag{12}$$

$$n_{paB} = \frac{n_{pss1B} - i_{0B} n_{pss2B}}{1 - i_{0B}} \tag{13}$$

where i_{0A} and i_{0B} are the basic speed-ratios of the planetary gear trains *A* and *B*, respectively. By substituting Eqs. (7) and (8) into Eq. (13), the following equation can be yielded as

$$n_{paB} = \frac{\beta n_{pss1A} - i_{0B} \alpha n_{paA}}{1 - i_{0B}} \tag{14}$$

By referring to Eq. (9) and equating Eqs. (12) and (14), the formulas for designing the practical arrangement of the ICT mechanism can be obtained as

$$\begin{cases} i_{0A} = \dfrac{\alpha - \beta}{\beta(\alpha - 1)},\ i_{0B} = \dfrac{\beta - 1}{\alpha - 1} & \text{if } \alpha \neq \beta, \alpha \neq 1 \text{ and } \beta \neq 1 \\ i_{0A} = 1 - i_{0B} & \text{if } \alpha = \beta = 1 \end{cases} \tag{15}$$

In addition, according to Eq. (9), it also concludes

$$N_{cmg2E} = N_{cmg3E} \tag{16}$$

4. Demonstrations of Prototypes of ICT Mechanisms

In this section, according to the design formulas about the practical arrangement of the ICT mechanism obtained previously, two prototypes of the proposed ICT mechanisms are assembled for experiments. From the results of the experiments, the correctness of the derived formulas and their feasibility in engineering applications can be shown and demonstrated, respectively.

A. Prototype 1: $\alpha \neq \beta$, $\alpha \neq 1$, *and* $\beta \neq 1$

In this prototype, as shown in Fig. 6, the constant multiples shown in Eqs. (7) and (8) are chosen to be $\alpha = 3$ and $\beta = 2$, respectively. Then, according to Eq. (15), the basic speed-ratios of the two sets of planetary gear trains *A* and *B* can be obtained as $i_{0A} = 0.25$ and $i_{0B} = 0.5$, respectively. By referring to Eqs. (7), (10), (11), and (16), the teeth numbers of the corresponding gears in this ICT mechanism can be chosen as listed in Table 1.

Figure 7 shows an actual test-bed of the ICT prototype in experiment, and Fig. 8 is the diagram about the angular velocities of the rotational shafts, including the input power, the output power, the controller, and the free end shafts, which are collected in the experiment. From the observation of Fig. 8, it can be found out that the magnitude of the angular velocities of the controller shaft, depicted by green dash line, is always 2 times of that of the output power shaft, depicted by red line, since their constant multiple β is chosen to be equal to 2, regardless of the variations of the angular velocities of the input power shaft, depicted by blue dash-dot line.

Table 1. Teeth numbers of corresponding gears in prototype 1.

Gear	*cmg1D*	*cmg2D*	*cmg3D*	*cmg1E*	*cmg2E*	*cmg3E*	*ps1A*
Teeth number	120	120	40	120	80	80	30
Gear	*ps2A*	*pp1A*	*pp2A*	*ps1B*	*ps2B*	*pp1B*	*pp2B*
Teeth number	15	15	30	40	30	20	30

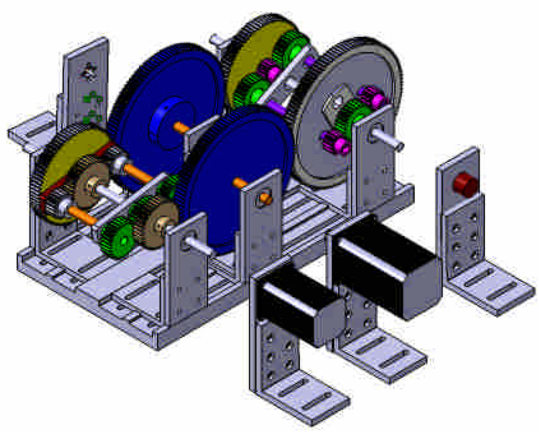

Fig. 6. Prototype 1 of ICT mechanism.

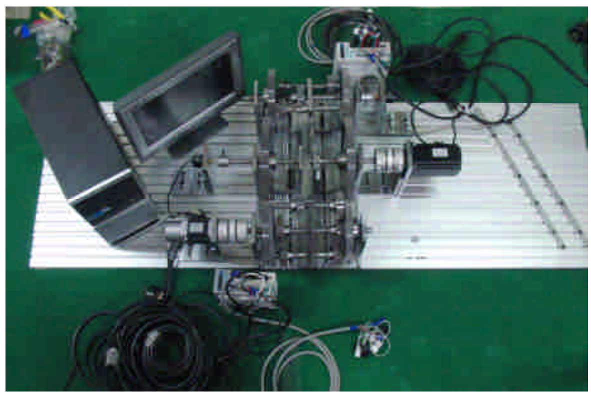

Fig. 7. An actual test-bed of ICT prototype.

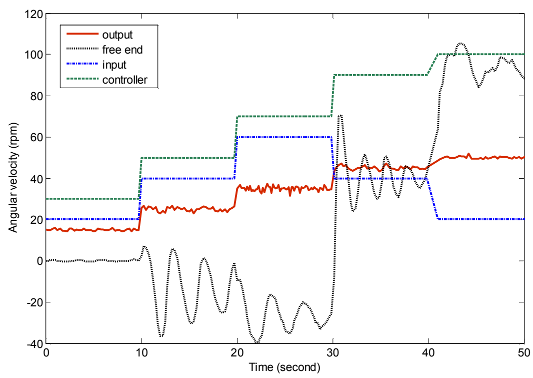

Fig. 8. Angular velocities of the rotational shafts in prototype 1 of ICT mechanism.

B. Prototype 2: $\alpha = \beta = 1$

In this prototype, as shown in Fig. 9, the constant multiples shown in Eqs. (7) and (8) are $\alpha = \beta = 1$. Also according to Eq. (15), the basic speed-ratio of the planetary gear trains *A* is chosen to be $i_{0A} = 0.5$, then the basic speed-ratio of the planetary gear trains *B* will be $i_{0B} = 1 - i_{0A} = 0.5$. Similarly, with referring to Eqs. (7), (10), (11), and (16), the teeth numbers of the corresponding gears in this ICT mechanism can be chosen as listed in Table 2.

Figure 10 is also the diagram about the obtained angular velocities of the rotational shafts in the experiment. It can be observed that the magnitude of the angular velocities of the controller shaft is always similar to that of the output power shaft, since their constant multiple β is chosen to be equal to 1, regardless of the variations of the angular velocities of the input power shaft.

From the results obtained in the above two prototypes, the correctness of the design formulas and feasibility of the proposed ICT mechanisms with steady-speed outputs are demonstrated.

Table 2. Teeth numbers of corresponding gears in prototype 2.

Gear	*cmg1D*	*cmg2D*	*cmg3D*	*cmg1E*	*cmg2E*	*cmg3E*	*ps1A*
Teeth number	80	80	80	120	40	40	40
Gear	*ps2A*	*pp1A*	*pp2A*	*ps1B*	*ps2B*	*pp1B*	*pp2*B
Teeth number	30	20	30	40	30	20	30

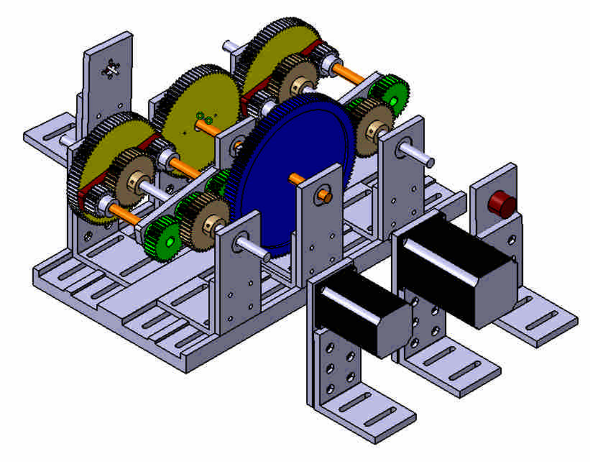

Fig. 9. Prototype 2 of ICT mechanism.

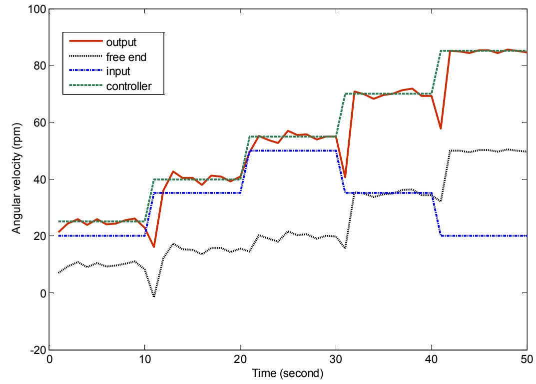

Fig. 10. Angular velocities of the rotational shafts in prototype 2 of ICT mechanism.

5. Conclusion

In this study, the innovative ICT mechanism with steady-speed outputs is proposed. In addition, the correctness of the design formulas and the feasibility in practical engineering applications of the proposed ICT mechanism are also demonstrated. Since the ICT mechanism can produce a steady-speed at the output power shaft, which is independently manipulated by a controller and completely not affected by the fluctuant speed of the input power shaft, such an ICT mechanism can be utilized in the variable speed wind turbines to generate the electric power with constant frequency. The further researches about the practical applications of the ICT mechanisms are continuously proceeding, and the patents of the ICT mechanisms are applied.

Acknowledgement

The financial support of the National Science Council of Taiwan under the grants (NSC 97-2221-E-110-031-MY2, NSC 98-3114-E-110-002) is gratefully acknowledged.

References

[1] J. Cotrell, "Motion technologies CRADA CRD-03-130: Assessing the potential of a mechanical continuously variable transmission," NREL/TP-500-36371, 2004.

[2] A. D. Şahin, "Progress and recent trends in wind energy," Progress in Energy and Combustion Science, 2004, Vol. 30(5), pp. 501-543.

[3] M. Pucci and G. Vitale, "High performance VOC-FOC based wind generator system with induction machine," Electric Machines and Drives Conference, 2009, pp. 1474 – 1479.

[4] H. Sharma, T. Pryor and S. Islam, "Effect of pitch control and power conditioning on power quality of variable speed wind turbine generators," Australasian Universities Power Engineering Conference, 2001, Perth, Australia, pp. 95-100.

[5] F. D. Bianchi, R. J. Mantz and C. F. Christiansen, "Power regulation in pitch-controlled variable-speed WECS above rated wind speed," Renewable Energy, 2004, Vol. 29(11), pp. 1911-1922.

[6] B. Boukhezzar, L. Lupu, H. Siguerdidjane and M. Hand, "Multivariable control strategy for variable speed, variable pitch wind turbines," Renewable Energy, 2007, Vol. 32(8), pp. 1273-1287.
[7] L. Mangialardi and G. Mantriota, "Dynamic behavior of wind power systems equipped with automatically regulated continuously variable transmission," Renewable Energy, 1996, Vol. 7(2), pp. 185-203.
[8] M. Idan and D. Lior, "Continuous variable speed wind turbine: Transmission concept and robust control," Wind Engineering, 2000, Vol. 24(3), pp. 151-167.
[9] X. Zhao and P. Maiβer, "A novel power splitting drive train for variable speed wind power generators," Renewable Energy, 2003, Vol. 28(13), pp. 2001-2011.
[10] D. F. Lahr and D. W. Hong, "The operation and kinematic analysis of a novel cam-based infinitely variable transmission," ASME International Design Engineering Technical Conferences & Computers and Information in Engineering Conference, 2006, DETC2006-99634.
[11] H. Müller, M. Pöller, A. Basteck, M. Tilscher and J. Pfister, "Grid compatibility of variable speed wind turbines with directly coupled synchronous generator and hydro-dynamically controlled gearbox," Sixth Int'l Workshop on Large-Scale Integration of Wind Power and Transmission Networks for Offshore Wind Farms, 2006, Delft, NL, pp. 307-315.
[12] H. W. Müller, Epicyclic Drive Trains - Analysis, Synthesis, and Applications, Wayne State University Press, Detroit (1982).